Bioelectromagnetics 33:238–246 (2012)

Altered Development of *Xenopus* Embryos in a Hypogeomagnetic Field

Wei-chuan Mo,[1,2] Ying Liu,[1,2]* Helen M. Cooper,[3] and Rong-qiao He[1,2]*

[1]*State Key Laboratory of Brain and Cognitive Science, Institute of Biophysics, Chinese Academy of Sciences, Chaoyang District, Beijing, China*
[2]*Graduate University of Chinese Academy of Sciences, Shijingshan District, Beijing, China*
[3]*Queensland Brain Institute, University of Queensland, Brisbane, Queensland, Australia*

The hypogeomagnetic field (HGMF; magnetic fields <200 nT) is one of the fundamental environmental factors of space. However, the effect of HGMF exposure on living systems remains unclear. In this article, we examine the biological effects of HGMF on the embryonic development of *Xenopus laevis* (African clawed frog). A decrease in horizontal third cleavage furrows and abnormal morphogenesis were observed in *Xenopus* embryos growing in the HGMF. HGMF exposure at the two-cell stage, but no later than the four-cell stage, is enough to alter the third cleavage geometry pattern. Immunofluorescent staining for α-tubulin showed reorientation of the spindle of four-cell stage blastomeres. These results indicate that a brief (2-h) exposure to HGMF is sufficient to interfere with the development of *Xenopus* embryos at cleavage stages. Also, the mitotic spindle could be an early sensor to the deprivation of the geomagnetic field, which provides a clue to the molecular mechanism underlying the morphological and other changes observed in the developing and/or developed embryos. Bioelectromagnetics 33:238–246, 2012.

Key words: geomagnetic field; embryonic development; malformation; spindle reorientation

INTRODUCTION

The geomagnetic field (GMF), which is produced by the dynamo action in the inner core of the Earth [Herndon, 2009], shields against cosmic rays that are hostile to living systems. The environmental magnetic field present in outer space is extremely low relative to the GMF and is termed a hypogeomagnetic field (HGMF). Besides greater cosmic radiation, the health of astronauts would be under potential risk due to exposure in the HGMF environment of space, given the longer duration of manned space missions [Yamashita et al., 2004], since it has been well established that the elimination of the GMF interferes with normal functions of life in many ways [Kopanev et al., 1979; Dubrov, 1989].

Early literature revealed that long-term exposure to HGMFs can disturb physiological and biochemical processes in rat cells [Shust and Kostinik, 1975, 1976; Levina et al., 1989; Borodin and Letiagin, 1990; Sandodze et al., 1995], and that brief (<2 h) exposures to HGMFs can induce transient hypercondensation of chromatin [Belyaev et al., 1997]. It has been reported that a 5-day HGMF exposure at the initial developmental stages has an adverse effect on newt embryonic development [Asashima et al., 1991]. For mouse primary embryos, HGMF exposure induces reorganization of the cytoskeleton, disturbs blastomere orientation, and inhibits embryonic development in vitro [Osipenko et al., 2008]. However, the mechanisms behind these biological responses to HGMF exposure remain unclear.

In this article, we extensively examined the effects of an HGMF (magnetic fields <200 nT) on the early embryonic development of *Xenopus laevis*

Additional Supporting Information may be found in the online version of this article.

Grant sponsor: Foundation of Chinese Academy of Sciences for Innovation projects (Ying Liu 2008-09), and the QCAS Biotechnology Fund (Grant No. GJHZ1131).

*Correspondence to: Ying Liu and Rong-qiao He, State Key Laboratory of Brain and Cognitive Science, Institute of Biophysics, Chinese Academy of Sciences, 15 Datun Road, Chaoyang District, Beijing 100101, China.
E-mail: liuy@moon.ibp.ac.cn; herq@sun5.ibp.ac.cn

Received for review 14 October 2010; Accepted 22 July 2011

DOI 10.1002/bem.20699
Published online 18 August 2011 in Wiley Online Library (wileyonlinelibrary.com).

(an African clawed frog generally used as a model for vertebrate embryonic development), especially at early cleavage stages. The results revealed that in the HGMF, the percentage of malformed embryos increased and the third cleavage geometry was altered, correlating with the change in the spindle orientation angles of four-cell stage blastomeres. These results suggest that a brief (2 h) HGMF exposure is enough to interfere with early cleavage stage development of *Xenopus* embryos and that the mitotic spindle could be an early sensor of the elimination of the GMF.

MATERIALS AND METHODS

Hypogeomagnetic Incubation Conditions

Two hypogeomagnetic incubation environments were utilized in this study. One is a $2 \times 3 \times 2$ m^3 magnetic shielding room (MSR; <200 nT) that was constructed with six layers of permalloy (magnetic permeability = 20,000, Beijing Shougang, Beijing, China) by the Biogeomagnetism Group of the Institute of Geology and Geophysics, Chinese Academy of Sciences (Beijing, China). The temperature in the MSR was 18.8 ± 0.8 °C, controlled by an air conditioner and monitored by a thermometer. Embryos were placed on a wooden shelf at the center of the MSR ($50 \times 50 \times 50$ cm^3). Geomagnetic control embryos (~22 μT) were incubated at 19.1 ± 0.2 °C in a thermostatic incubator (Model GXZ-160, Ningbo Jiangnan Instrument, Ningbo, China), monitored by a internal thermo-probe outside the MSR.

The second hypogeomagnetic incubation environment utilized a Helmholtz coil system (HCS; <150 nT), as described previously [Wang et al., 2008]. The controls were incubated on the same platform (separated by 20 cm, ~52 μT) to ensure similar environmental conditions for samples in the HCS, except for the magnetic field. The temperature in the laboratory was set at 19.0 ± 2.0 °C. The direct current (DC) magnetic field was measured with a three-axis fluxgate magnetometer (Model 520, Applied Physics Systems, Mountain View, CA). The sum of alternating current (AC) noise fields was measured using a CCG-1000 induction alternative magnetometer (National Institute of Metrology, Beijing, China), and the predominant AC field frequency was checked from the output of signal on a Tektronics TDS 2014 digital real-time oscilloscope (Tequipment.NET, Long Branch, NJ). The detailed magnetic field conditions are listed in Table 1.

Embryo Manipulation

Xenopus embryos were prepared according to a previously published in vitro fertilization protocol [Sive et al., 1997]. Embryos were cultured in 100 mm Petri dishes (no more than 200 and 50 embryos per dish before and after stage 20, respectively) with 0.1X Marc's Modified Ringers (MMR) solution (10 mM NaCl, 0.2 mM KCl, 0.2 mM $CaCl_2$, 0.1 mM $MgCl_2$, 0.5 mM Hepes, pH 7.4) at 19 °C.

For experiments in the MSR, adult frogs were cultured in the HGMF and GMF for 1 week before fertilization. Immediately after fertilization, embryos

TABLE 1. Magnetic Field Conditions for the Incubation of *Xenopus* Embryos

DC magnetic field	$\|B\|$	B_X[a]	B_Y[b]	B_Z[c]
Magnetic shielding room (nT)	104.9 ± 12.6	66.7 ± 7.1	−44.4 ± 14.2	65.6 ± 15.1
GMF control (incubator, μT)	22.0 ± 1.6	12.7 ± 1.6	−11.6 ± 3.7	1.3 ± 0.3
Helmholtz coils (nT)[d]	65.6 ± 14.8	40.0 ± 27.5	16.0 ± 29.5	26.7 ± 34.5
GMF control (μT)	52.5 ± 0.4	24.5 ± 0.2	−8.1 ± 0.0	45.8 ± 0.6
AC magnetic field		$\|B\|_{Ac}$[e](nT)		Frequency (Hz)[f]
Magnetic shielding room		8.2 ± 0.4		132.2 ± 29.9
GMF control (incubator)		263.3 ± 5.8		62.9 ± 5.4
Helmholtz coils[g]		12.8 ± 1.0		131.7 ± 21.9
GMF control		14.0 ± 0.0		157.3 ± 19.2

Data are mean ± SD of three measurements in the same location but at different times.
[a]Positive direction of the *X*-axis is pointing from south to north.
[b]Positive direction of the *Y*-axis is pointing from west to east.
[c]Positive direction of the *Z*-axis is pointing vertically downward.
[d]Hypogeomagnetic field in the coils system can remain stable for 6 h.
[e]Net AC magnetic field (the vector sum of the three directions).
[f]Predominant frequency in all experimental environments was 50 Hz.
[g]Data were obtained when the coils system was at the HGMF condition.

were divided and cultured in the MSR (>30 embryos per experiment) or the control incubator (>10 embryos per experiment). Embryos from different fertilizations were taken as independent experimental samples. The number of embryos in each experiment depended on the amount of eggs produced each time. After a 2- or 4-day incubation period, embryos were collected and fixed, and phenotypes of embryos in each experiment group were analyzed.

For experiments in the HCS, embryos were prepared and cultured in the GMF before being divided and transferred into the HGMF or the control GMF at the stage indicated. Embryos of the exposed and control groups were derived from the same fertilizations and run at the same time. All experimental procedures involving animals were performed in accordance with the Institutional Code of Ethics.

Phenotype Analysis

Embryos were collected and fixed in MOPS/EGTA/magnesium sulfate/formaldehyde buffer (MEMFA) solution (100 mM 3-(*N*-Morpholino)propanesulfonic acid (MOPS), 2 mM ethylene glycol tetraacetic acid (EGTA), 1 mM $MgSO_4$, 4% formaldehyde, pH 7.4) for 1 h at room temperature and stored in 100% ethanol at −20 °C. Embryonic stages were determined as previously described [Nieuwkoop and Faber, 1994; Bowes et al., 2009]. The aberrant morphogenesis on axis disturbance was classified according to the standard dorsoanterior index (DAI) as previously described [Sive et al., 1997]. The anomalies not included in the DAI, such as double heads, bubbled belly, cyclopia, and coloboma, are very easily identified phenotypes. Eye reduction was measured as described by Qiu et al. [2009]. To avoid biased observation, all the phenotypes described were identified by two or three scientists in our lab without the knowledge of the exposure conditions. Images were taken using a stereomicroscope DP71 CCD camera (Olympus SZH16, Tokyo, Japan). Malformation percentages of day-2 and -4 embryos were calculated as the percentage of total embryos in each group that displayed abnormal phenotypes.

Cleavage Analysis

Eight-cell stage embryos were collected and fixed in MEMFA solution. At least 30 embryos were collected in each experimental group. Cleavage was defined as horizontal if the angle between the cleavage furrow and the embryo equator was <30°. Eight-cell embryos were classified into five types according to the number of horizontal cleavage furrows (0–4) in each embryo. The horizontal cleavage index is defined as the average number of third cleavage furrows per embryo. The horizontal cleavage index is calculated as [Denegre et al., 1998; Valles et al., 2002]:

$$\frac{\sum_{i=0}^{4} Ni \times i}{\sum_{i=0}^{4} Ni}$$

where i is the number of horizontal cleavage furrows in an embryo, and Ni is the number of embryos grouped by the number "i." Images were taken as described above.

Immunofluorescent Staining

Embryos were fixed in 100% methanol for 1 h at the four-cell stage and stored at −20 °C. Fixed embryos were cut along the second cleavage furrow and processed for immunofluorescent staining as previously described [Valles et al., 2002]. Microtubules were detected using a mouse anti-α tubulin antibody (Thermo Labvision, Fremont, CA), diluted 1:200 in PBS with 0.1% Tween-20 (PBS/T20). A secondary antibody, Cy-3-labeled donkey anti-mouse IgG (Jackson ImmunoResearch, West Grove, PA), was applied and diluted 1:500 in PBS/T20. Chromosomes were stained with SYTOX green nucleic acid stain (Sigma, St. Louis, MO) diluted 1:50. After washing twice with PBS/T20, embryos were dehydrated in 100% methanol and cleared in Murray's clear (1:2, benzyl alcohol: benzyl benzoate) for imaging. Images were taken using an inverted fluorescence microscope (Olympus IX71) with the Olympus DP71 CCD camera.

Measurement of Spindle Orientation Angle

The spindle orientation angle (θ) is defined as the angle between the major axis of the spindle and that of the first two cleavage furrows [Valles et al., 2002]. Four-cell stage blastomere θ values were measured on the immunofluorescent images at 15° intervals. We defined an index sum of angle as: $S_{\theta[a,b]} = \sum\theta, \theta \in [a, b]$, that is, the sum of the angle values within an angle range [a,b]. The distribution of spindle orientation angles was evaluated by the sum of the spindle angle percentage: $S_{\theta[a,b]}/S_{\theta[0,90]} \times 100\%$, which takes into account not only the frequency but also the values of the angle for each blastomere.

Statistical Analysis

The Student's t-test was used for the malformation and spindle angle analysis, and the chi-square test for data of the cleavage experiments summed

from three independent experiments. Means are calculated from three independent experiments and expressed as mean ± standard deviation (SD), unless specified otherwise. Differences were considered to be significant when $P < 0.05$.

RESULTS

Abnormal Morphogenesis of *Xenopus* Embryos in the Hypogeomagnetic Field (HGMF)

In order to observe the effect of HGMF on the early development of *Xenopus laevis*, the MSR was used for a long-term continuous HGMF exposure. Eggs were obtained from frogs pre-exposed in the MSR and embryos were incubated in the MSR immediately after fertilization. The results of phenotype analysis after 2 and 4 days of exposure showed that more abnormal morphogenesis was observed in the HGMF (Fig. 1, Online Table 1), although the embryonic mortalities in the HGMF and the control groups were the same (data not shown). At the tailbud stage (stage 26, day 2), strong aberrant phenotypes such as double heads, bubbled belly, and twisted spine were distinguishable and became more clear at tadpole stages (Fig. 1F–I). The malformation percentage in the HGMF group was 8.0 ± 1.5%, significantly higher than that in the control group (2.6 ± 2.5%, $P = 0.04$; Fig. 1J, Online Table 1). When embryos grew to day 4 (tadpole stages 40–46), more anterior anomalies such as eye reduction, coloboma, and cyclopia were found (Fig. 1A–C). The percentage of malformed embryos in the HGMF-treated group reached 27.3 ± 8.0%; however, in the GMF control group it was only 6.9 ± 1.2%, and thus much lower ($P = 0.01$; Fig. 1J, Online Table 1).

These results indicate that HGMF exposure can induce abnormal morphogenesis of *Xenopus laevis* during embryonic development.

Decrease of Horizontal Third Cleavage Furrows in the HGMF

To map the early timing of the above effects, as well as to examine the effects of short-term HGMF exposure on *Xenopus* development, exposed embryos at cleavage, blastula, gastrula, and neurula stages were also collected in the MSR, following the sampling strategy described above with >30 embryos in each independent group. Compared with the GMF control group, embryos in the HGMF group showed no significant morphological changes during these early stages (data not shown), except for the third cleavage (eight-cell stage).

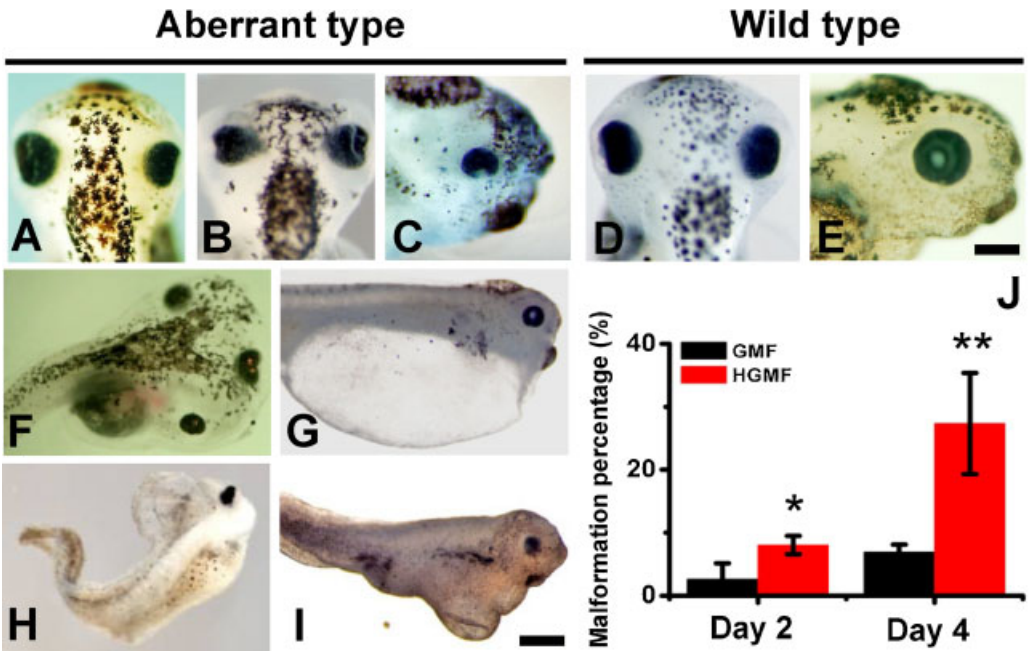

Fig. 1. Malformation of *Xenopus* embryos in the hypogeomagnetic field (HGMF). Embryos with representative anomalies were incubated and photographed at tadpole stages. **A**–**E**: Dorsal (A,B,D) and lateral (C,E) views of heads of embryos with anterior defects: eye reduction (A), cyclopia (B), and coloboma (C); and the wild-type (D,E). **F**–**I**: Aberrant trunk phenotypes: double-headed (F), bubbled belly (G), twisted spine (H), and abnormal gastrointestinal development (I). Bar = 0.5 mm (A–E) or 1.25 mm (F–I). **J**: Malformation percentage of day-2 and -4 embryos in HGMF (MSR) and GMF. Error bar = SD; $^{*}P < 0.05$, $^{**}P < 0.01$. [Color figure can be seen in the online version of this article, available at http://wileyonlinelibrary.com/journal/bem]

For *Xenopus* embryo cleavage, the first two orthogonal cleavage furrows are both vertical to the embryo equator, dividing the embryo into four blastomeres along the animal–vegetal (A–V) axis. The third cleavage furrow is usually perpendicular to the first two cleavage furrows (A–V axis) and horizontal to the equator of the embryo; however, non-horizontal third cleavage furrows can sometimes be observed. Thus, eight-cell embryos can be classified into five types according to the number of horizontal cleavage furrows (0–4; Fig. 2A). However, in the HGMF the pattern of third cleavage geometry was notably altered.

For eight-cell stage embryos in the HGMF group, no more than one-quarter of the total embryos ($23.8 \pm 4.6\%$) were type 3 and 4, compared with over one-third ($38.7 \pm 5.6\%$) in the GMF group (Fig. 2B, Online Table 2), indicating that fewer horizontal cleavages were formed in the HGMF. The horizontal cleavage index showed that the average horizontal cleavage number in the HGMF group (1.86 ± 0.08) was smaller than that in the GMF control group (2.06 ± 0.07; Fig. 2B, Online Table 2). A chi-square test showed that the cleavage patterns in the HGMF and GMF groups were significantly different ($P = 0.03$).

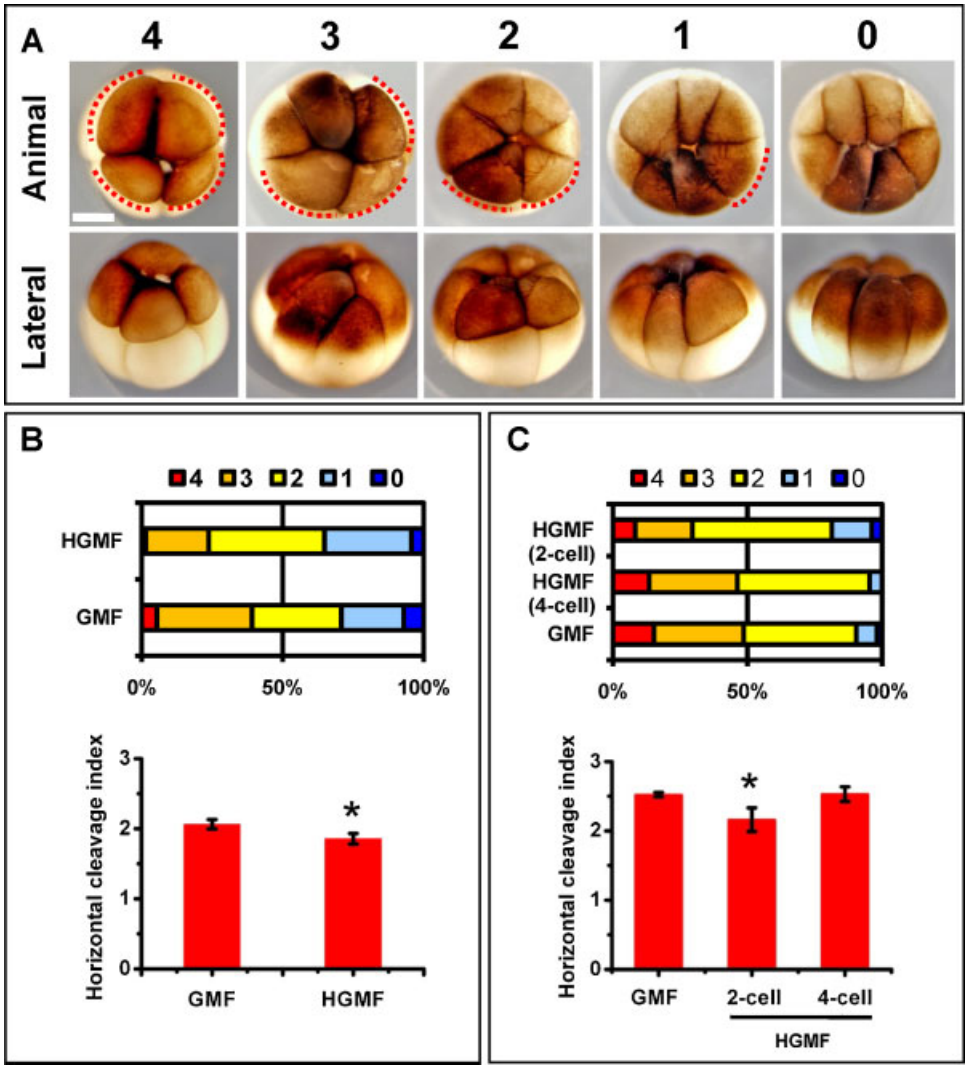

Fig. 2. **A**: Third cleavage geometries of *Xenopus* embryos shown from animal and lateral views of eight-cell *Xenopus* embryos. Red dashed arcs indicate the position of horizontal cleavage furrows. Bar = 0.3 mm. **B**,**C**: Bar-clustered graphs illustrate the distribution of five cleavage patterns, and the column graphs show the horizontal cleavage index of embryos in the HGMF and GMF groups from experiments in the MSR (B) or the HCS (C). Error bar = SD; $^{*}P < 0.05$. [Color figure can be seen in the online version of this article, available at http://wileyonlinelibrary.com/journal/bem]

These results indicate that the developmental geometry, or the positioning map of the developing blastomeres, were changed at the very beginning of the developmental process due to a few hours of HGMF exposure (from fertilization to the eight-cell stage, <2 h).

Alteration of the Third Cleavage in the HGMF Is Stage Dependent

We further applied HGMF exposure to cleavage stage embryos to determine whether the alteration of the third cleavage geometry in the HGMF was stage dependent using the HCS. This technique is more convenient than the MSR for the treatment manipulation and provides more standardized environmental conditions between the control and exposed samples in the absence of the GMF.

Embryos fertilized in the GMF were transferred into the HCS at the two-cell or four-cell stage, and fixed at the eight-cell stage for cleavage analysis as described above. The sampling strategy was the same as the experiments in the MSR with >30 embryos in each independent dish. Eight-cell embryos collected in the GMF were taken as control (~52 μT). As shown in Figure 2C and Online Table 2, the ratio of type 3 and type 4 embryos in the two-cell HGMF group (29.7 ± 8.3%) was lower than that for the GMF group (48.6 ± 2.7%). The ratio of type 3 and type 4 embryos in the four-cell HGMF group (45.9 ± 7.9%) was similar to that of the control. This analysis also showed that the horizontal cleavage index of the two-cell HGMF group was smaller than that of the four-cell HGMF and GMF control groups. The chi-square test showed that there was no significant difference in cleavage patterns between the GMF group and the four-cell HGMF group. However, statistical significance was demonstrated between the two-cell HGMF group and the other two groups ($P = 0.03$ for the GMF group; $P = 0.002$ for the four-cell HGMF group). Moreover, when we applied 1 μT magnetic exposure to the embryos in the HCS from the two-cell stage to the eight-cell stage, no significant change was observed on the horizontal cleavage index either (data not shown).

These results show that the effect of HGMF exposure (in the HCS) on cleavage geometry is stage dependent. During the period from the beginning of the first cleavage (two-cell) to the end of the third cleavage (eight-cell), the HGMF exposure in the first half of this time interval, about 1 h, is crucial to the formation of the third cleavage pattern of the eight-cell embryo, indicating that the biological events that occur before the end of the second cleavage (four-cell stage) are closely related to the biological response to HGMF exposure.

Spindle Reorientation in *Xenopus* Embryos in the HGMF

Because the direction of the third cleavage furrow is perpendicular to the spindle orientation of the four-cell stage blastomere, we examined, by immunofluorescent staining, the spindle orientation angle (θ) of the four-cell embryos, which were put into the HCS or the control GMF at the two-cell stage. The θ

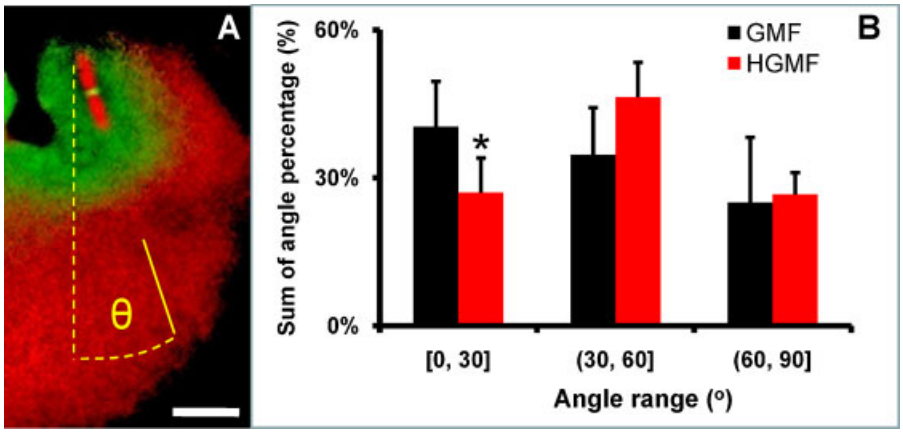

Fig. 3. Spindle orientation of *Xenopus* four-cell embryos in HGMF. **A**: Measurement of the spindle orientation angle in a blastomere of the four-cell embryo. The angle between the major axis of spindle (yellow line) and the axis of first cleavage furrow (yellow dashed line) was defined as the spindle orientation angle (θ) of each blastomere. Spindle (red) and chromosome (green) were shown by immunofluorescent staining. Bar = 0.3 mm. **B**: Distribution of spindle angles shown as percentages of the sum of spindle angles within the indicated ranges. Error bar = SEM; $^{*}P < 0.05$. [Color figure can be seen in the online version of this article, available at http://wileyonlinelibrary.com/journal/bem]

of each blastomere was measured (Fig. 3A) in 15° intervals (Online Table 3). We compared the percentage of embryos within each spindle angle range for the HGMF and GMF groups. We found that when the distribution of spindle angles was divided into three angle ranges, [0°, 30°], (30°, 60°], and (60°, 90°], as shown in Figure 3B, there was a smaller percentage of blastomeres with small spindle angles [0°, 30°] and a larger percentage with medium spindle angles (30°, 60°] in the HGMF group compared to those in the GMF control group (the square bracket means the marginal value is included in the range, while the parenthesis is not). The percentage of blastomeres in the HGMF group with very large spindle angles, (60°, 90°] was similar to that found in the GMF control group. Comparison of the angles in the range of [0°, 30°] showed that the sum percentages of spindle angles for embryos in the HGMF group was significantly lower than that for the GMF control group ($P = 0.025$). This observation correlates with the change in the horizontal cleavage index due to the HGMF.

These results further confirm that the HGMF exposure (in the HCS) affects the cleavage of *Xenopus* embryos by altering the orientation of the mitotic spindle apparatus and suggest that the mitotic spindle may be a sensor for the change in the local magnetic field.

DISCUSSION

In this article, we report a comprehensive morphological analysis of *Xenopus* embryo development, from fertilization to the completion of organogenesis, in the HGMF (in the MSR). During HGMF exposure of up to 4 days, we found that percentages of abnormal embryos increased from tailbud to tadpole stages, suggesting that the GMF contributes to maintaining normal embryonic development. The morphological changes in *Xenopus* embryos, including spinal curvature and intestinal protrusion, are similar to the abnormal phenotypes seen in newts subjected to pulsed HGMF exposure [Asashima et al., 1991]. Moreover, in addition to the anomalies in the trunk, we found that at tadpole stages the embryos also exhibited head defects, especially in the eyes (Fig. 1A–C,F), which are part of the central nervous system. Learning and memory dysfunction has been reported in *Drosophila* and chicks after continuous HGMF exposure [Xu et al., 2003; Zhang et al., 2004; Xiao et al., 2009]. Therefore, our finding provides additional evidence that continuous HGMF exposure can induce defects in the central nervous system.

In addition, we found that the third cleavage furrow of embryos exposed to HGMF (both in the MSR and HCS) is less horizontal compared to embryos exposed to normal GMF. In the HGMF, the spindle angle of four-cell stage blastomeres was larger in the HGMF (in the HCS), leading to the formation of more vertical furrows at the third cleavage. Cleavage is the initiating process of embryonic development, and the location of blastomeres of the cleaving embryos determines their cell fate during later differentiation [Chung et al., 1994]. Although we have not observed a direct correlation between the alteration in the third cleavage geometry and the type of malformation phenotype seen at later stages, it has been reported that altering the position of the first horizontal cleavage furrow of the *Xenopus* egg reduces embryonic survival [Yokota et al., 1992]. Thus, the malformation of embryos that we observed in the HGMF group may have resulted from the reduction in horizontal cleavage. Further analysis is required to determine whether the early change in cleavage geometry would imprint on the fine structure at cellular and molecular levels, as well as on the behavior of the developing and/or developed embryos. Another finding we obtained was the distinct effect of the HGMF (in the HCS) on early cleavage during a very short exposure time (within 2 h) from the two-cell stage to the eight-cell stage. These phenotypes are similar to those seen in longer exposures in the MSR. In most investigations on the biological effects of HGMFs, the exposure time of the HGMF, either in the MSR or in the HCS, is relatively long: 5 days for the newt [Asashima et al., 1991], 10 generations for *Drosophila* [Zhang et al., 2004], 22–24 days for chicks [Xu et al., 2003], and up to 60 days for golden hamsters [Zhang et al., 2007]. Therefore, this implies that a long exposure period is required for significant biological defects to appear. Our results suggest that a very brief HGMF exposure (<2 h) is sufficient to exert adverse influence on living systems. In particular, the events during the second cleavage are essential to the biological response at the third cleavage in the absence of the GMF.

Moreover, we confirmed that the change in the third cleavage geometry corresponds to the reorientation of mitotic spindles at the four-cell stage in the HGMF (in the HCS). The simple geometry of *Xenopus* embryos at the cleavage stage is a favorable model system for analyzing the effects of external forces on living systems [Chung et al., 1994; Denegre et al., 1998]. It has been reported that additional mechanical forces can alter the location or orientation of the cleavage furrow [Yokota et al., 1992; Chung et al., 1994; Akiyama et al., 2010]. The

alteration of cleavage geometry in the HGMF suggests that elimination of the GMF might disturb the balance of the inner forces that control the normal cleavage geometry of embryos. We have reported previously that the tubulin self-assembly reaction is disordered in the same HGMF (in the HCS) [Wang et al., 2008]. Tubulin assembly is the major driver of spindle formation. The dynamic stability of the microtubule is essential to many vital processes [Van der Vaart et al., 2009] including cell migration, cell differentiation, and neural plasticity. Thus, the sensitivity and rapid response of the microtubule structures to the reduction of the GMF might explain the effects of HGMFs on animal behavior. Our finding provides the first in vivo evidence to suggest that the microtubule system plays a role in sensing the presence of GMFs. Additionally, our findings provide new insights into the role of the GMF in biological systems. This is important since the GMF has been a ubiquitous environmental factor throughout evolution.

In addition, the MSR and the HCS were applied in this study to provide long-term and short-term exposures to HGMFs, respectively. As shown in Table 1, the static magnetic fields of both HGMFs were less than 150 nT, no more than 1/200 of their controls. The control magnetic field of the MSR (22.0 μT) was lower than that of the HCS control (52.5 μT) due to the shielding effect of the metal incubator. However, this level of magnetic field reduction did not significantly affect the incubated embryos since we found that the exposure to a much lower magnetic field (1 μT) led to no significant change in the horizontal cleavage index of two-cell stage to eight-cell stage embryos in the HCS (data not shown). We also noted the background AC noise fields in the experimental environments (Table 1), and found that the net magnetic induction and the frequency of the summed AC fields in the MSR (8.2 nT, 132.2 Hz), HGMF in the HCS (12.8 nT, 131.7 Hz), and GMF control (14.0 nT, 157.3 Hz) were almost identical, except in the control incubator for the MSR (263.3 nT, 62.9 Hz). Furthermore, the predominant frequencies of the AC fields in all experimental environments were 50 Hz, which is equal to the power line frequency in China. The relatively higher AC field in the control environment for the MSR is probably due to electrical components of the thermostatic incubator, suggesting that the control GMF samples from this environment may be affected. However, thermostatic incubators have been extensively used to control the developmental speed of *Xenopus* embryos [Nieuwkoop and Faber, 1994; Sive et al., 1997]. To date, no report has shown any disturbance in *Xenopus* embryonic development due to such incubators per se. The similar effects of MSR and HCS exposure on the third cleavage furrow of embryos also indicate that the differences between these two approaches did not influence the effects of GMF elimination, at least in our analysis of embryonic cleavage.

CONCLUSION

In summary, continuous HGMF exposure promotes abnormal morphogenesis at early stages of *Xenopus* embryonic development (in the MSR). A brief (<2 h) HGMF exposure is enough to induce a small but significant alteration in the third cleavage geometry at the eight-cell stage (both in the MSR and HCS), which could result from the reorientation of spindles at the four-cell stage (in the HCS). Therefore, the mitotic spindle could be an early sensor for the elimination of the GMF.

ACKNOWLEDGMENTS

We sincerely thank Yong-xin Pan from the Institute of Geometry and Geophysics, Chinese Academy of Sciences, for kindly providing the magnetic shielding room. We thank Wen-kui Jia for the measurement of the magnetic fields, and Dong-liang Wang and Xiu-mei Wang for technical assistance.

REFERENCES

Akiyama M, Tero A, Kobayashi R. 2010. A mathematical model of cleavage. J Theor Biol 264(1):84–94.

Asashima M, Shimada K, Pfeiffer CJ. 1991. Magnetic shielding induces early developmental abnormalities in the newt, *Cynops pyrrhogaster.* Bioelectromagnetics 12:215–224.

Belyaev I, Alipov YD, Harms-Ringdahl M. 1997. Effects of zero magnetic field on the conformation of chromatin in human cells. Biochim Biophys Acta 1336:465–473.

Borodin YI, Letiagin AY. 1990. Reaction of circadian rhythms of the lymphoid system to deep screening from geomagnetic fields of the earth. Biull Eksp Biol Med 109:191–193.

Bowes JB, Snyder KA, Segerdell E, Jarabek CJ, Azam K, Zorn AM, Vize PD. 2009. Xenbase: Gene expression and improved integration. Nucleic Acids Res 38 (Database issue): D607–D612. http://www.xenbase.org/xenbase/original/atlas/NF/NF-all.html (last accessed 20 January 2011).

Chung HM, Yokota H, Dent A, Malacinski GM, Neff AW. 1994. The location of the third cleavage plane of *Xenopus* embryos partitions morphogenetic information in animal quartets. Int J Dev Biol 38:421–428.

Denegre JM, Valles JM, Jr., Lin K, Jordan WB, Mowry KL. 1998. Cleavage planes in frog eggs are altered by strong magnetic fields. Proc Natl Acad Sci 95:14729–14732.

Dubrov AP. 1989. The geomagnetic field and life: Geomagnetobiology. New York: Plenum (translated from Russian by Sinclair FL).

Herndon JM. 2009. Nature of planetary matter and magnetic field generation in the solar system. Curr Sci 96:1033–1039.

Kopanev VI, Efimenko GD, Shakula AV. 1979. Biological effect of a hypogeomagnetic environment on an organism. Biol Bull Acad Sci USSR 6:289–298.

Levina RV, Smirnov RV, Olimpienko TS. 1989. Effect of a hypogeomagnetic field on warm-blooded animals. Kosm Biol Aviakosm Med 23:45–47.

Nieuwkoop PD, Faber J. 1994. Normal table of *Xenopus laevis* (Daudin). New York: Garland Publishing.

Osipenko MA, Mezhevikina LM, Krasts IV, Iashin VA, Novikov VV, Fesenko EE. 2008. Influence of ''zero'' magnetic field on the growth of embryonic cells and primary embryos of mouse in vitro. Biofizika 53:705–712.

Qiu R, Liu Y, Wu YJ, Liu K, Mo W, He R. 2009. Misexpression of miR-196a induces eye anomaly in *Xenopus laevis*. Brain Res Bull 79:26–31.

Sandodze V, Svanidze IK, Didimova EV. 1995. Effects of hypomagnetic fields on motility of the cilia of ependymal cells in vivo. Radiats Biol Radioecol 35:19–22.

Shust IV, Kostinik IM. 1975. Effect of a strong constant magnetic field and a hypomagnetic surrounding medium on histochemical indices of albino rat liver. Kosm Biol Aviakosm Med 9:19–25.

Shust IV, Kostinik IM. 1976. Reaction of the animal adrenal cortex to the action of a strong, constant magnetic field and to a hypomagnetic environment. Probl Endokrinol (Mosk) 22:86–92.

Sive HL, Grainger RM, Harland RM. 1997. Early development of *Xenopus laevis*, 5th edition. New York: Cold Spring Harbor Laboratory Press.

Valles JM, Jr., Wasserman SR, Schweidenback C, Edwardson J, Denegre JM , Mowry KL . 2002. Processes that occur before second cleavage determine third cleavage orientation in *Xenopus*. Exp Cell Res 274:112–118.

Van der Vaart B, Akhmanova A, Straube A. 2009. Regulation of microtubule dynamic instability. Biochem Soc Trans 37(Pt 5):1007–1013.

Wang DL, Wang XS, Xiao R, Liu Y, He RQ. 2008. Tubulin assembly is disordered in a hypogeomagnetic field. Biochem Biophys Res Commun 376:363–368.

Xiao Y, Wang Q, Xu ML, Jiang JC, Li B. 2009. Chicks incubated in hypomagnetic field need more exogenous noradrenaline for memory consolidation. Adv Space Res 44:226–232.

Xu ML, Wang XB, Li B, Li DF, Jiang JC. 2003. Long-term memory was impaired in one-trial passive avoidance task of day-old chicks hatching from hypomagnetic field space. Chinese Sci Bull 48:2454–2457.

Yamashita M, Tomita-Yokotani K, Hashimoto H, Takai M, Tsushima M, Nakamura T. 2004. Experimental concept for examination of biological effects of magnetic field concealed by gravity. Adv Space Res 34:1575–1578.

Yokota H, Neff AW, Malacinski GM. 1992. Altering the position of the first horizontal cleavage furrow of the amphibian (*Xenopus*) egg reduces embryonic survival. Int J Dev Biol 36:527–535.

Zhang B, Lu H, Xi W, Zhou X, Xu S, Zhang K, Jiang J, Li Y, Guo A. 2004. Exposure to hypomagnetic field space for multiple generations causes amnesia in *Drosophila melanogaster*. Neurosci Lett 371:190–195.

Zhang X, Li JF, Wu QJ, Li B, Jiang JC. 2007. Effects of hypomagnetic field on noradrenergic activities in the brainstem of golden hamster. Bioelectromagnetics 28:155–158.